

The effects of a tidal-mixing front on the distribution of larval fish habitats in a semi-enclosed sea during winter

EMILIO A. INDA-DÍAZ^{1,2}, LAURA SÁNCHEZ-VELASCO² AND MIGUEL F. LAVÍN^{3†}

¹Universidad Autónoma de Nayarit, Ciencias Biológicas, Agropecuarias y Pesqueras, Km. 9 Carretera Tepic-Compostela, Xalisco, Nayarit, México 63780, ²Centro Interdisciplinario de Ciencias Marinas, Avenida Instituto Politécnico Nacional s/n, Col. Playa Palo de Sta. Rita, La Paz, B.C.S., México 23000, ³Centro de Investigación Científica y de Educación Superior de Ensenada, Carretera Ensenada-Tijuana 3918, Zona Playitas, Ensenada, Baja California, México 22860

*We examined the effect of a tidal-mixing front on the three-dimensional distribution of larval fish habitats (LFHs) in the Midriff Archipelago Region in the Gulf of California during winter. Zooplankton and environmental variables were sampled from 0 to 200 m in 50 m strata. Four LFHs were defined in association with the front, two on the northern side and two on the southern side. The northern LFHs were: (1) the Mainland Shelf Habitat, located from the surface to 100 m depth on the north-east mainland shelf, characterized mainly by the presence of *Citharichthys fragilis*; and (2) the Wide Distribution Habitat, extending from north-west to south across the front from the surface to 200 m depth, dominated by the ubiquitous *Engraulis mordax*. The southern LFHs were: (3) the Eddy Zone Habitat, defined nearly on an anticyclonic eddy, with the highest larval abundance and richness from the surface to 100 m depth, dominated by *Leuroglossus stilbius*; and (4) the Southern Gulf Habitat, associated with low temperature waters from the southern Gulf of California, dominated by southern-gulf species (e.g. *Scomber japonicus* and *Sardinops sagax*). Despite the weak stratification and low thermal contrast ($\sim 1.5^{\circ}\text{C}$) across the south front compared to summer ($\sim 3^{\circ}\text{C}$), our results demonstrate that the frontal zone may influence the formation of planktonic habitats even during generally homogeneous periods, which may also be relevant in other regions of the world.*

Keywords: larval fish habitat, tidal front, mesoscale oceanographic processes, anticyclonic eddy, three-dimensional distribution, Gulf of California, Mexico

Submitted 11 December 2012; accepted 27 January 2014; first published online 1 May 2014

INTRODUCTION

Physical oceanographic processes are highly influential in regulating the horizontal and vertical distribution of pelagic fish eggs and larvae on a variety of scales, ranging from a few meters to thousands of kilometres (Doyle *et al.*, 1993; Bruce *et al.*, 2001). The coupling between fish species spawning and mesoscale hydrographic structures, such as eddies, meanders and fronts, may increase larval survival (Iles & Sinclair, 1982), as these structures act as mechanisms for enrichment, concentration and retention of nutrients and planktonic organisms (e.g. fish larvae and their prey) (Bakun, 1996). In particular, frontal zones are characterized by elevated productivity due to convergence processes in the surface layer (Moser & Smith, 1993). In these systems, contiguous planktonic habitats may occur within short distances (Sánchez-Velasco *et al.*, 2009), resulting in larval fish habitats (LFHs) with different hydrographic characteristics (e.g. Moser & Smith, 1993; Costello, 2009; Danell-Jimenez *et al.*, 2009; Contreras-Catala *et al.*, 2012).

Most studies on relationships between LFHs and mesoscale processes, such as frontal zones, have described physical–

biological interactions in the vertically integrated upper 200 m (i.e. using bongo nets). A minor number of studies described the vertical distribution of LFHs (i.e. collected by opening–closing nets) related to frontal zones. For example, Moser & Smith (1993) studied the vertical distribution of fish larvae in a frontal zone in the eastern Pacific ocean off Ensenada, Mexico, and found different patterns of vertical distribution for the same species north and south of the front, related to stratification of the water column. John *et al.* (2001) found higher zooplankton biomass, as well as higher fish larval abundance and diversity in the most stratified layer on the warm side of the Angola–Benguela frontal system. However, how the physical structures influence the three-dimensional distribution of LFHs, especially under low-stratified environmental conditions, are not yet understood, despite the importance for the fish larvae survival and their ecological repercussions on the pelagic ecosystem.

In the Gulf of California (GC), a highly dynamic and productive semi-enclosed sea (Alvarez-Borrego & Lara-Lara, 1991; Lavín & Marinone, 2003), several mesoscale processes promote the enrichment and transport of nutrients and plankton (including fish eggs and larvae) in the upper ocean layers (Danell-Jiménez *et al.*, 2009; Sánchez-Velasco *et al.*, 2009; Inda-Díaz *et al.*, 2010; Contreras-Catala *et al.*, 2012). One of the most relevant hydrographic features of the GC is the area of permanent minimum sea surface

Corresponding author:

Emilio A. Inda-Díaz
Email: eindad@uan.edu.mx

temperature (SST) around the islands of the Midriff Archipelago Region (MAR; Figure 1). This low SST is due to intense tidal mixing over the San Lorenzo and San Esteban Sills, and to upwelling in the Ballenas Channel, induced by the convergence of deep water at the subsurface over the sills at both ends of the channel (Paden *et al.*, 1991; Argote *et al.*, 1995; López *et al.*, 2006). The cool area is limited in the south and north by thermal fronts, which frequently show convolutions, eddies and filaments that spread the low SST and nutrients around the MAR (Paden *et al.*, 1991; Navarro-Olache *et al.*, 2004; Sánchez-Velasco *et al.*, 2009). During summer, a strong pycnocline is formed at ~20 m depth resulting in multi-variable environmental gradients through the water column, forming several environmentally distinct habitats. In winter, strong

north-westerly winds generate vertical mixing and cooling-induced convection, creating a mixed layer that can reach 100 m depth. The seasonal circulation is highly predictable in the GC, and especially in the northern GC, being cyclonic during summer and anticyclonic during winter. As a consequence of the overall seasonal circulation scheme, the coastal circulation in the eastern coast of the MAR is north-westward in summer and south-eastward in winter (Marinone, 2003; Peguero-Icaza *et al.*, 2011). In the MAR there are no major riverine outflows, only minor sporadic seasonal runoffs, while in the southern GC there are larger outflows off the mainland, but not large enough to affect the circulation (Martínez *et al.*, 2011). These seasonal differences in the vertical structure of the water column and circulation suggest possible changes in the physical–biological interactions.

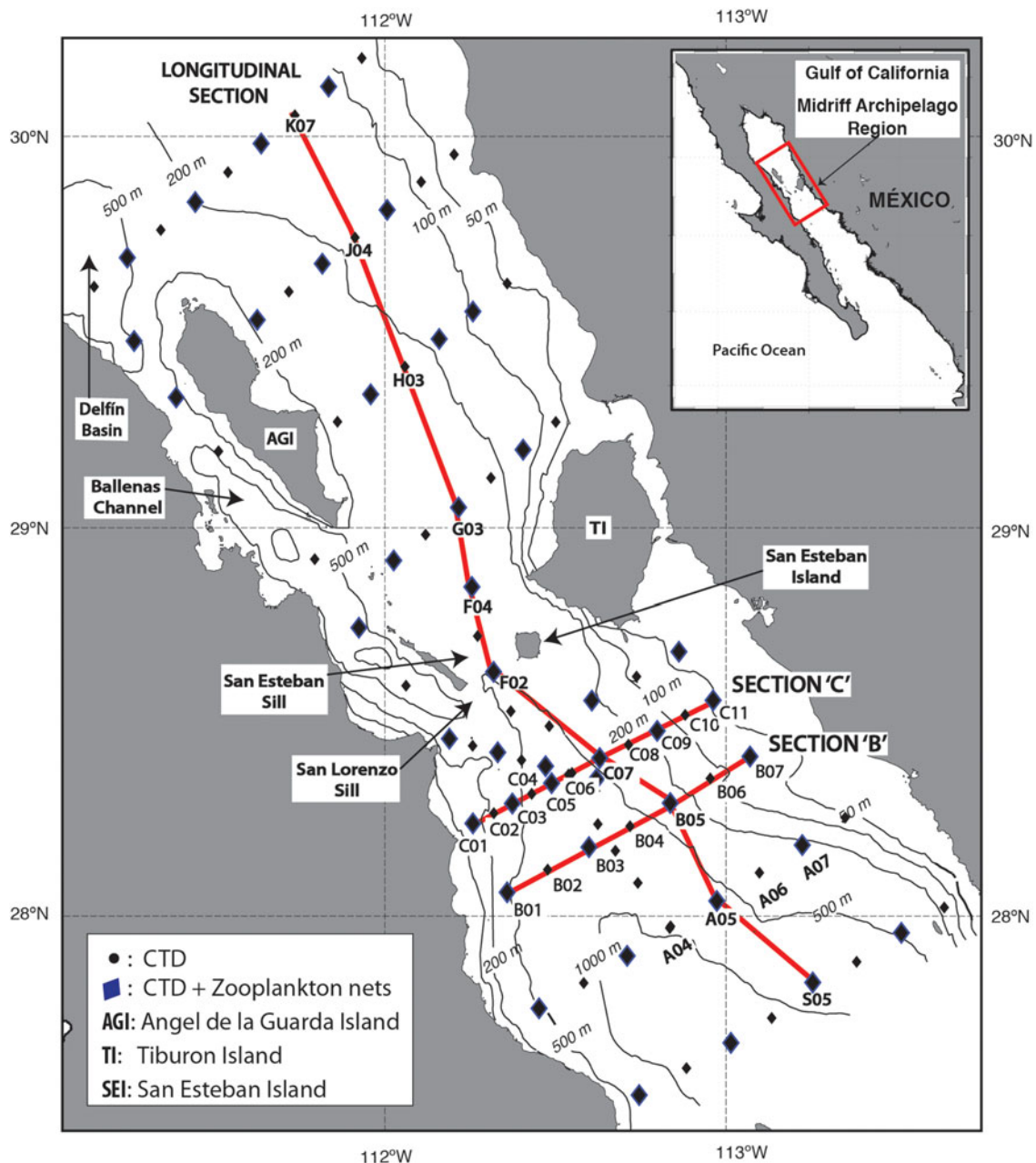


Fig. 1. The study site (Midriff Archipelago Region; MAR) in the Gulf of California, Mexico. Location, main geographical features (islands, channels and sills), and bathymetry contour lines (depth in metres). Lines indicate selected longitudinal and transversal sampling transects (Longitudinal Section, Sections 'C' and 'B') presented in Figures 3 and 4. Black circles indicate conductivity, temperature and depth (CTD) samples, diamonds CTD and zooplankton samples.

There are two previous studies on the effects of physical processes on the vertical distribution of fish larvae in the frontal zone of the GC, performed during two contrasting seasons. The first study was conducted in summer, a season of strong environmental gradients. It showed that the thermal front and the thermocline functioned as horizontal and vertical boundaries, respectively, with profound effects on the three-dimensional distribution of fish larvae (Danell-Jiménez *et al.*, 2009). The front as a vertical barrier (SST difference $\sim 3^{\circ}\text{C}$) separated two main larval habitats: one on the warm side of the front, dominated by six species (e.g. *Auxis* spp. and *Syacium ovale* Günther, 1864), and one on the cold side of the front dominated by *Benthoosema panamense* (Tåning, 1932) (Danell-Jiménez *et al.*, 2009). The second study was conducted in winter, when the surface thermal front south of the MAR was much weaker than in summer (SST difference $\sim 1.5^{\circ}\text{C}$). Nevertheless, it acted differentially on the two species studied: as a barrier down to 100 m depth for preflexion and flexion larvae of the south-distributed species *Sardinops sagax* (Jenyns, 1842), whereas flexion larvae of *Engraulis mordax* (Girard, 1854) were found on both sides of the front in the entire water column (Inda-Díaz *et al.*, 2010). The differential response of these species suggests that weak thermal fronts may have distinct effects on the larval distribution of different fish species. This previous knowledge raises the question of how the tidal-mixing frontal system of the GC influences the whole fish larvae community under low-stratified environmental conditions.

We hypothesize that the differential spawning and response of fish larvae species to weak environmental gradients in the thermal frontal system during the winter, and the mesoscale hydrographic structures associated to the front, define contiguous LFHs. The aim of this study is to find out if the tidal-mixing front located in the MAR of the GC and associated mesoscale hydrographic structures contribute to the three-dimensional distribution of LFHs during winter (February 2007). The results of this study will contribute on the knowledge about LFH definition under conditions of strong mixing and weak environmental gradients.

MATERIALS AND METHODS

Physical and zooplankton data were obtained from 19 February to 1 March 2007, during the GOLCA-0702 campaign on-board of the RV 'Francisco de Ulloa'. For detailed information about the cruise refer to García-Córdova *et al.* (2007). The grid of 90 stations, designed with the aid of SST images from the Moderate Resolution Imaging Spectroradiometer (MODIS) aboard the Terra and Aqua satellites (4 km \times 4 km resolution), covered a wide area of the MAR, from north of Angel de la Guarda Island to San Pedro Mártir Basin in the south (Figure 1).

Physical variables

Temperature, conductivity and dissolved oxygen profiles were obtained at each station with a SeaBird 911plus conductivity, temperature and depth (CTD) profiler. Surface mixed layer depth was defined as the depth where temperature was 0.8°C lower than at the surface (Martínez-Sepúlveda, 1994). Geostrophic velocity was calculated based on the geopotential anomaly, obtained from objectively mapped potential

temperature (θ) and practical salinity distributions. We integrated the specific volume anomaly from the 150 m reference level to the surface to avoid the effect of subsurface (200–350 m depth) density undulations that may be due to internal waves or internal tides common in this area.

Lagrangian surface currents were measured with two surface drifters with a 10 m holey sock centred at 15 m, and tracked with the Advanced Research and Global Observation Satellite (ARGOS) satellite telemetry system. The data were quality-controlled and interpolated at 6 h intervals by the Global Drifter Program of the National Oceanic and Atmospheric Administration (NOAA) as described by Hansen and Poullain (1996).

Three vertical sections (Section 'B', Section 'C' and Longitudinal Section in Figure 1) were selected to illustrate the vertical thermal and haline structure, as well as geostrophic velocity across the study area.

Zooplankton sampling

Zooplankton samples were obtained using opening-closing conical zooplankton nets (60 cm mouth diameter, 250 cm length, and 505 μm mesh size) with a calibrated General Oceanics flow meter attached to the mouth (<http://www.generaloceanics.com>). We performed oblique hauls both day and night at four depth-strata (200–150 m, 150–100 m, 100–50 m and 50–0 m) at 39 of the 90 stations. As strata were of the same depth, two strata were sampled simultaneously during each haul, placing two closed nets separated by 71.5 m distance. The distance between nets and the depth for each stratum was calculated by the cosine of the wire angle method following the standard specifications of Smith & Richardson (1977). The closed nets were lowered to the bottom of the stratum to be sampled, opened with a manual brass messenger, and then the haul was started. When the upper level of the sampling stratum was reached, the nets were closed with a second messenger and the haul ended. This system effectively avoids contamination of the sample with organisms from other strata. This stratified sampling technique has been successfully applied in several previous studies (e.g. Sánchez-Velasco *et al.*, 2007; Danell-Jiménez *et al.*, 2009; Inda-Díaz *et al.*, 2010). The volume of filtered water was calculated using the flow meter placed at the mouth of each net.

Samples were fixed in 5% formalin buffered with sodium borate. Fish larvae were separated from zooplankton samples and identified according to the descriptions of Moser (1996). Their abundance was standardized to number of larvae per 10 m^2 according to Smith & Richardson (1977).

Data analysis

In order to verify if there were statistically significant differences in larval fish abundance (total and for the most abundant species) between day and night, and among strata, the non-parametric Kruskal–Wallis (K-W) test was applied due to the non-normal distribution of data tested with the Kolmogorov–Smirnov test (Sokal & Rohlf, 2012).

To determine the presence of distinct LFHs in the MAR, we applied a cluster analysis based on the species abundance matrix (Clarke & Ainsworth, 1993) of samples from all strata. Rare species, i.e. species contributing less than 10% to the total abundance and with a frequency of < 3 , were excluded, in order to consider only the most representative

species of the study area. An agglomerative dendrogram was created based on a triangular similarity matrix (Bray–Curtis similarity index; Sokal & Rohlf, 2012), using complete–average linkage on fourth-root transformed larval abundance data to minimize the effect of outlier values (Field *et al.*, 1982). The cut line in the dendrogram was chosen visually, according to common practice in zooplankton and fish larvae studies (e.g. Doyle *et al.*, 1993; Moser & Smith, 1993).

To detect significant differences among distinct LFHs, we applied a multi-response permutation procedure (MRPP; McCune & Grace, 2002). Based on the triangular similarity matrices, the MRPP compares average intra-group distances with all other possible combinations of the entire dataset under the null hypothesis of no group structure. To identify the species that: (1) contributed most to the similarity within groups; and (2) accounted most for differences between close groups, we applied a similarity percentage test (SIMPER) using the PRIMER 6.0 software (Clarke & Ainsworth, 1993).

In order to characterize each LFH several ecological indices were calculated (Clarke & Warwick, 2001). Simpson's index of dominance (λ) was calculated to assess if one or a few species dominated the community. λ assesses the probability that any two individuals, chosen at random from the sample, belong to the same species; high values correspond to assemblages whose total abundance is dominated by one or by very few species. The Shannon–Weaver index (H') was calculated to assess the diversity level and the evenness of species distribution. It calculated the probability in predicting the species of an individual chosen at random from a collection of S species and N individuals. The average probability decreases as the number of species increases and is lowest when all species are equally abundant (Mijail, 2004).

To analyse and determine if the LFH distribution has any relationship with the environmental variables, a step-wise distance-based linear model (DISTLM) with R^2 selection criteria was applied (Anderson *et al.*, 2008). This test has a semi-parametric permutation-based approach that does not assume a set of normal distributed data. It is a form of multivariate multiple regression over a distance or dissimilarity matrix it can also be used to analyse partial (conditional) tests, where the amount of variation explained by a given predictor variable is determined after other variables have been fitted into the model (Anderson *et al.*, 2008). The resulting models are visualized graphically on a biplot obtained through a redundancy analysis (db-RDA) that runs an eigen analysis and produces a constrained ordination of the predictor variables responsible for explaining significant portions of the variation within the data cloud. The DISTLM has been used widely on community ecology studies (Heagney *et al.*, 2007; Trumpickas *et al.*, 2011; Leduc *et al.*, 2012; Siver & Lott, 2012).

Finally, distinct maps of the LFHs were drawn for each of the four strata to illustrate their three-dimensional distribution and overlaid on maps of the physical variables to illustrate the relation between LFHs and their potential environmental boundaries.

RESULTS

Physical structure

The surface distributions (upper 10 m averages) of temperature, salinity and dissolved oxygen are shown in Figure 2A–C; the density distribution was very similar to that of temperature

and, therefore, is not shown. Surface temperature (Figure 2A) was $\sim 16.5^\circ\text{C}$ in the north-eastern shelf, $\sim 15.5^\circ\text{C}$ south of Ballenas Channel and $\sim 17^\circ\text{C}$ in the south of the study area. We observed several surface thermal fronts around the cool area created by tidal mixing and upwelling in Ballenas Channel and around Angel de la Guarda island; the sharpest front ('the south front' henceforth) was located between the Baja California peninsula coast and San Esteban Island (marked as a thick dashed line in Figure 2). Surface salinity was highest in the northern sector (35.4) due to high evaporation in the northern GC, lowest in Ballenas Channel (35.1) over San Lorenzo Sill (which is due to mixing in a water column where salinity decreased with depth, as is the case in the GC) and intermediate in the south (around 35.2) (Figure 2B). There were haline surface fronts around the low-salinity area, and the strongest was, again, the south front. Surface dissolved oxygen (Figure 2C) was highest in the north zone (6 ml/l) due to winter vertical convection in the northern GC, and lowest in the strong tidal mixing zones around the sills (3.5–4 ml/l), associated with the minima in temperature and salinity, and delimited by the south front. In the south-east (south of the frontal zone), there was an isolated area of very low dissolved oxygen (4.5 ml/l).

The surface mixed layer reached ~ 80 m depth in the north, and its maximum depth (~ 100 m) in the tidal-mixing area of minimum surface temperature, salinity and dissolved oxygen (Figure 2D) northwest of the south front. In the north-eastern shelf, the mixed layer was only ~ 40 m deep. South of the frontal zone, mixed layer depth was generally ~ 40 m, except for an isolated anomaly (80 m maximum depth) in the south-east ($\sim 28.2^\circ\text{N}$, $\sim 112.3^\circ\text{W}$) enclosed by the 50 m isoline, coinciding with the isolated low oxygen zone mentioned above. The geopotential anomaly relative to 150 m showed the strongest gradient across the southern frontal zone, between low values over the strong mixing zone north of the front ($\sim 2.6 \text{ m}^2/\text{s}^2$) and high values in the south ($\sim 3 \text{ m}^2/\text{s}^2$) (Figure 2E). This implies a north-westward jet parallel to the front. The highest geopotential anomaly ($3.1 \text{ m}^2/\text{s}^2$) was measured in the same area as the deep mixed layer anomaly south of the front, which suggested the presence of an anticyclonic eddy.

The surface currents measured by the drifters are shown in Figure 2E, as arrows superimposed on the geopotential anomaly. The south drifter (set at the south-west limit of the minimum temperature zone, empty arrows in Figure 2E) initially followed the frontal jet north-westwards (12 h mean speed 0.07–0.47 m/s), and then turned anticyclonically along the northern and eastern edges of the anticyclonic eddy. In the northern part of the study area, the geopotential anomaly suggested a weak northward flow, but the north drifter (filled arrows in Figure 2E) showed a southward flow (12 h mean speed 0.01–0.33 m/s), veering westwards in front of Tiburon Island. The southward flow and its westward deflection were congruent with the surface temperature and salinity distribution patterns (Figure 2B). For this reason we defined the southern limit of the northern zone approximately in the area where the north drifter (filled arrows) veered west, just north of the minimum temperature/salinity mixing area. The thermohaline properties of the study area suggested the presence of three main hydrographic domains: (1) the north zone (intermediate temperature and high salinity values); (2) the tidal-mixing area delimited by the southern front

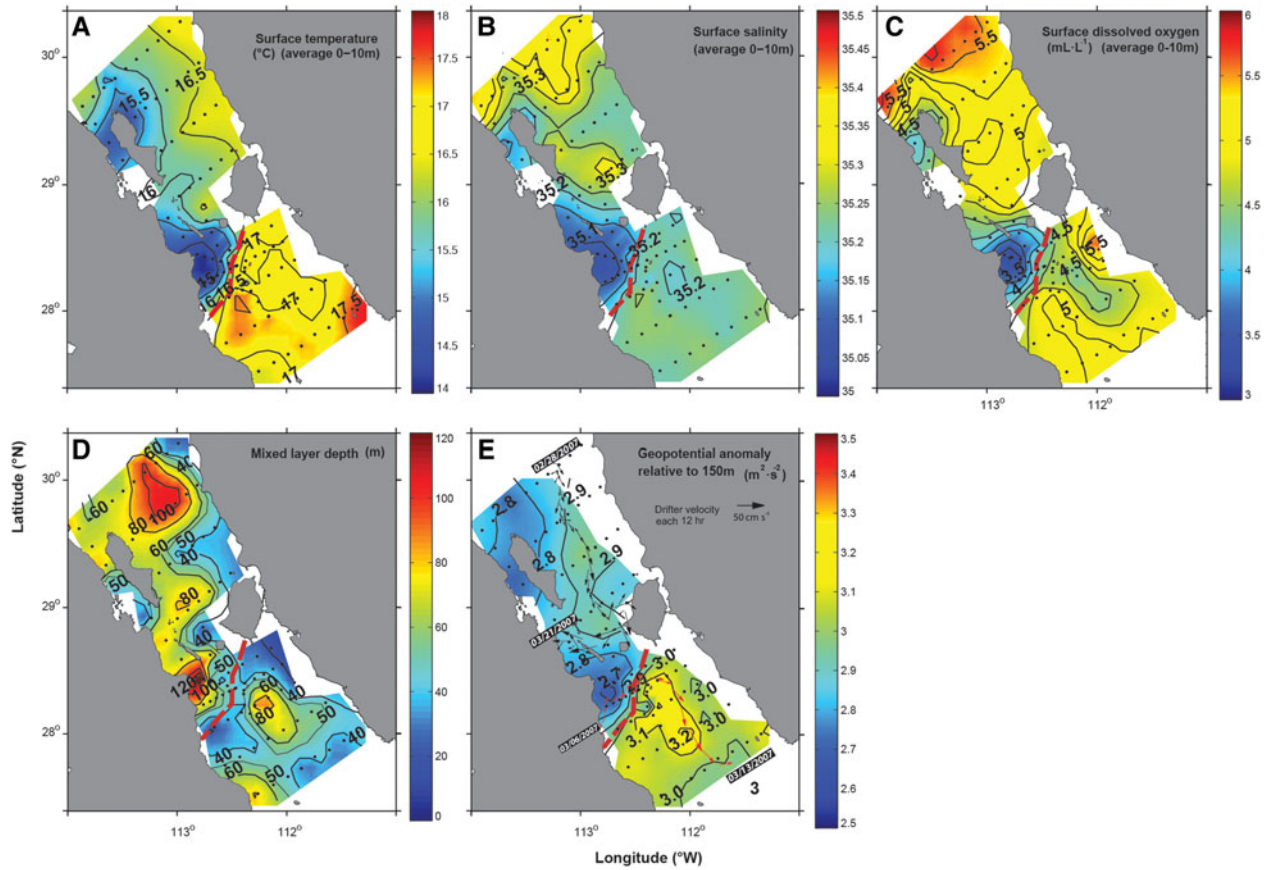


Fig. 2. Values at the time of sampling of: (A) temperature ($^{\circ}\text{C}$, 0–10 m depth average); (B) salinity (0–10 m depth average); (C) dissolved oxygen (mL/L , 0–10 m depth average); (D) mixed layer depth (m); (E) geopotential anomaly relative to 150 m (m^2/s^2). Arrows indicate directions and velocities of drifters set in the northern part of the study area in February (filled arrows) and in the south in March (empty arrows) each 12 h. The thick dashed line indicates the position of the south front.

(minimum temperature, salinity and dissolved oxygen); and (3) the south zone (high temperature and low salinity values).

The vertical distribution of temperature in a section crossing the south front (Section ‘C’ in Figure 1) showed that the thermal south front between the southern limit of the strong-mixing zone north of the front (Stations Co1–Co3) and the more stratified area (15°C at ~ 60 m vs 17°C at the surface) south of the front was formed by the outcropping of the 15°C – 17°C isotherms between stations Co3 and Co6 (Figure 3A). This outcropping was due to the break-up of stratification at stations Co1 and Co2 and further north by tidal mixing. The 15°C isotherm was lifted from 100 m depth to the surface in only 30 km. The 14°C isotherm was lifted from 175 m depth in the deep area to 50 m depth in the mixing zone (Co1 and Co2). The geostrophic velocity relative to 150 m (colours, Figure 3A) showed a 100 m deep geostrophic jet at the position of the front, with a maximum velocity of ~ 0.25 m/s at the surface. This was the velocity component normal to Section ‘C’ (i.e. north-westwards), but in reality the jet had a northward direction, along the thermal front.

The western end of Section ‘B’ (Figure 3B) almost reached the southern edge of the front (Figure 1). Isotherms did not reach the surface, but the tilt of the 15°C – 17°C isotherms between stations Bo1 and Bo3 produced a geostrophic flow (~ 0.15 m/s) that was composed of the frontal effect on the one hand, and the western side of the eddy on the other.

The eddy was made evident by the bowl shape of the 15°C and 16°C isotherms centred on station Bo4 (Figure 3B). On the eastern side, south-eastward flow (~ 0.1 m/s) was present between Stations Bo5 and Bo6, that was part of the anticyclonic eddy circulation.

From the curvature of the isotherms and the geostrophic velocity distribution in Figure 3B it was observed that the eddy was approximately centred on Bo4. We estimated visually that the eddy had a diameter of $\sim 50 \pm 7.5$ km, from midway between Bo2 and Bo3 to midway between Bo5 and Bo6; with a swirl speed ~ 0.10 – 0.15 m/s, its rotation time was 12–18 d. It is unfortunate that the formation and evolution of this eddy were not observed, because the satellite images before, during and after the cruise were very poor due to cloud coverage.

The subsurface hydrographic structure along the Longitudinal Section showed the characteristics of the three main hydrographic domains: the south zone, the tidal-mixing area limited by fronts, and the north zone (Figure 4). In the south zone, thermal stratification was present (15°C at ~ 60 m vs 17°C at the surface) although weaker than in summer, when surface temperatures exceed 30°C . The surface thermal front was approximately identified by the 16°C isotherm reaching the surface (Stations Fo2–Co7; Figure 4A). In the strong tidal-mixing area over San Esteban Sill (Station Fo2), nearly well mixed conditions prevailed in the upper 150 m. The undulations of the deeper isotherms

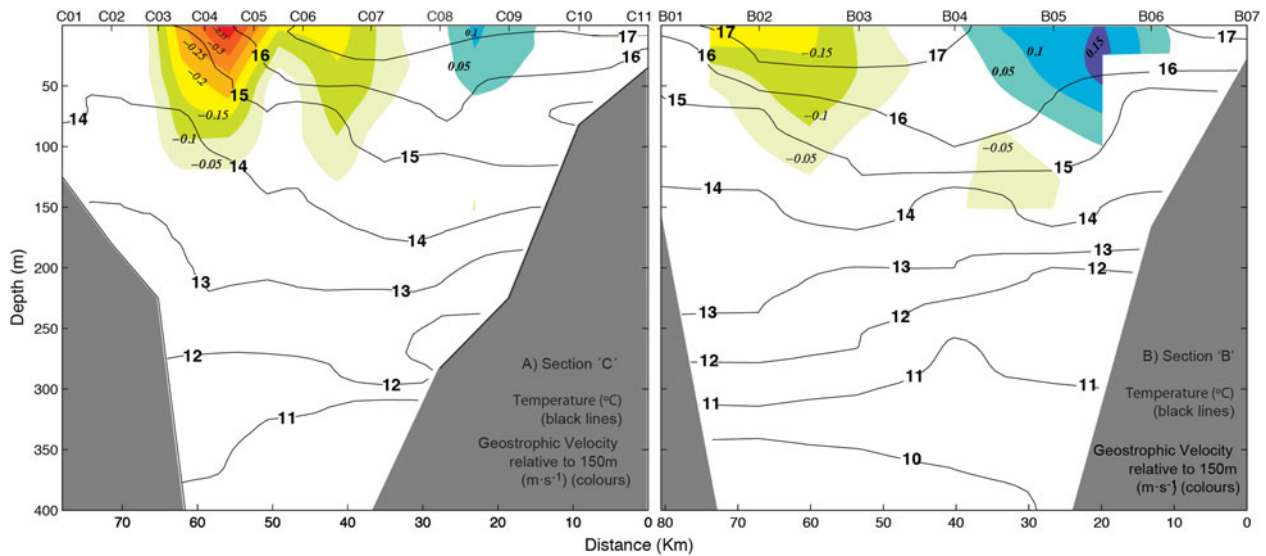


Fig. 3. Vertical profiles of temperature ($^{\circ}\text{C}$; isolines) and geostrophic velocity (m/s relative to 150 m; gray tones) along (A) Section 'C', and (B) Section 'B'.

were probably due to internal waves or internal tides. Salinity was highest (35.3) in the mixed layer of the north zone and lowest (35.15) over San Esteban Sill (Figure 4B). The density anomaly distribution showed the 26 kg/m^3 isopycnal tilting toward the surface on both sides of the strong mixing area (Station F02; colours of Figure 4C). This isopycnal tilting caused a north-eastward geostrophic jet on the southern side of the front and a weaker south-westward flow on the

northern side. The weaker flows between Stations B05, A05 and S05 were related to the anticyclonic eddy.

Fish larvae community characterization

A total of 107 zooplankton samples were analysed and 11,708 fish larvae from 36 taxa were separated and identified (>90% preflexion and flexion larvae); the taxonomic list is presented in Supplementary Material I. A total of 25 families were registered. Families represented by a high number of taxa were Myctophidae (four taxa), Paralichthyidae, Scorpenidae and Sebastidae (three taxa each). The most abundant species were *Engraulis mordax* (mean larval abundance: 318.9 ± 29 larvae/ 10 m^2), *Leuroglossus stilbius* (Gilbert 1890; 237.8 ± 20 larvae/ 10 m^2), *Diogenichthys laternatus* (Garman 1899; 77.3 ± 12 larvae/ 10 m^2), *Sardinops sagax* (46.0 ± 8 larvae/ 10 m^2) and *Citharichthys fragilis* (Gilbert 1890; 14.3 ± 4 larvae/ 10 m^2). A total of 19 taxa had temperate or temperate-subtropical affinity, and 17 had tropical or tropical-subtropical affinity. Twenty taxa were of demersal adult habits, six were coastal pelagic, and 10 had mesopelagic adult habits (Supplementary Material I; Moser & Smith, 1993; Aceves-Medina et al., 2004).

There were no statistically significant differences between day and night (K-W test, $P > 0.5$) in total larval abundance and *E. mordax* abundance (the most abundant and frequent species of the study), neither were there statistically significant differences among strata (K-W test, $P > 0.5$), although tendencies towards lower larval abundances in deeper strata were observed.

Larvae were present in the entire study area, with two distinct high-abundance spots (Figure 5). The first was observed north of Angel de la Guarda Island in the 0–50 m stratum, with ~ 300 larvae/ 10 m^2 associated with low species richness and diversity (Figure 5A, E). At this site, no such high abundance was observed in deeper strata (Figure 5B–D). The second high abundance site (~ 250 larvae/ 10 m^2) was located south of the surface thermal front. It was characterized by high species richness (>20 taxa) and diversity ($H' = \sim 2.5$), with maximum values between the front and the eddy, and

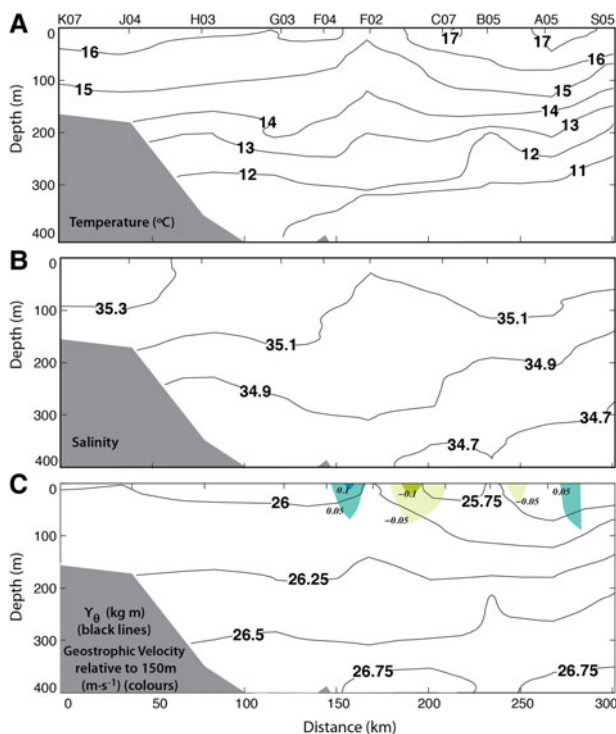


Fig. 4. Vertical profiles of (A) temperature ($^{\circ}\text{C}$), (B) salinity, and (C) potential density anomaly relative to 150 m (m^2/s^2 ; isolines) and geostrophic velocity relative to 150 m (m/s ; grey tones), along the Longitudinal Section (see Figure 1).

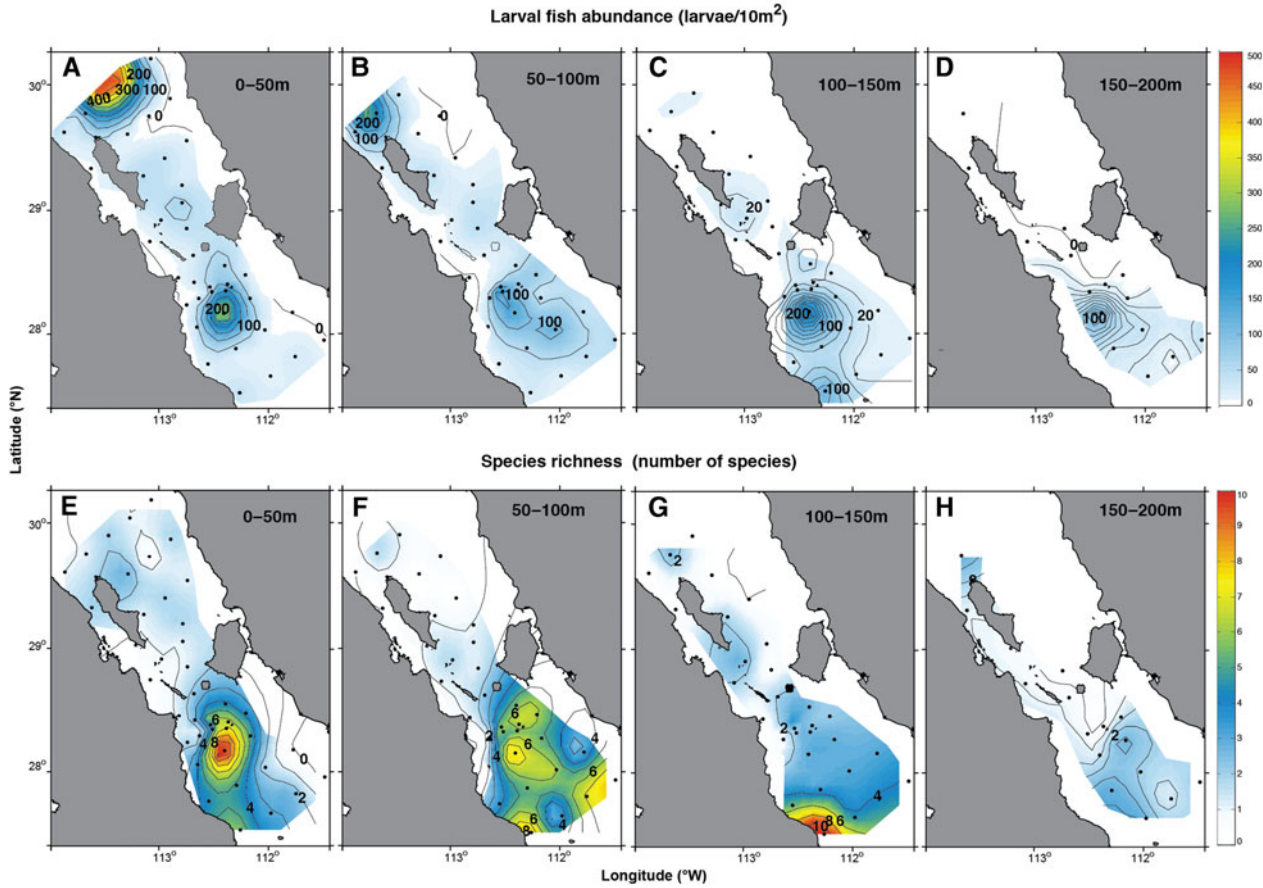


Fig. 5. Fish larval abundance (larvae/10 m²; A–D) and species richness (i.e. number of species; E–H) in 50 m depth intervals from 0 to 200 m.

inside the eddy. Below 50 m depth, the abundance and diversity decreased gradually (Figure 5D, H).

Identification of four larval fish habitats

Four LFHs were identified according to a 20% cut line in the dendrogram (Figure 6). The MRPP test showed significant differences among these LFHs based both on the fish larvae species presence/abundance ($T = -35.577984, A = 0.29983241, P < 0.05$) and on diversity indices of each habitat ($T = -3.0457362, A = 0.04983799, P < 0.05$). The SIMPER test showed high dissimilarities among LFHs (Supplementary Material II).

The distance-based linear model based on all samples identified that environmental variables each by themselves explained part of the variation in LFH distribution (salinity $R^2 = 0.132 P = 0.001$, dissolved oxygen $R^2 = 0.109 P = 0.001$, temperature $R^2 = 0.029 P = 0.023$, mixed layer depth $R^2 = 0.070 P = 0.003$). And when the best combination on variables is fitted, a total 29.3% of the variance is explained statistically significant just by salinity ($R^2 = 0.131 P = 0.001$), temperature ($R^2 = 0.232 P = 0.001$) and dissolved oxygen ($R^2 = 0.29 P = 0.0001$). From the total explained variation the 26% was explained on the axis 1 (85.2% of the fitted model), and 2.8% on the axis 2 (9.2% of the fitted model) (Table 1).

The relation between samples belonging to different LFH and the environmental variables could be observed graphically in the db-RDA ordination shown on Figure 7. Samples of

every habitat were distributed in all strata so it could be found in a wide range of dissolved oxygen conditions. The Mainland Shelf Habitat was found in typical northern gulf waters with high salinity and a deeper mixed layer. Like the Southern Gulf Habitat, the Eddy Zone Habitat samples were found in lower salinity and warmer waters from the southern gulf; however the latter had a distribution in lowest oxygen and deepest mixed layer zones. The Wide Distribution Habitat reached several different environmental conditions.

The three-dimensional distribution of LFHs is shown in Figure 8. The four habitats were named after their relation to physical-topographical associations. Two of the LFHs were located north of the south front and the other two south of it.

MAINLAND SHELF HABITAT

The first LFH in the north, named the Mainland Shelf Habitat (Figure 8), contained 14 samples located mainly from the surface to 100 m depth. It was composed of six taxa, including the widespread epipelagic *E. mordax* (Supplementary Material III A–D) and the demersal *C. fragilis* (Supplementary Material III E–H). Average similarity among samples was 65.3% (SIMPER, Table 2). *Engraulis mordax* contributed 54.5% to the group definition with a mean abundance of 199.05 larvae/10 m², *C. fragilis* contributed 44% with 11.98 larvae/10 m² (both species with widespread distributions in the north zone), and the Mainland Shelf Habitat-exclusive *Merluccius productus* (Ayres, 1855) contributed 1.1% with 3.10 larvae/10 m². This

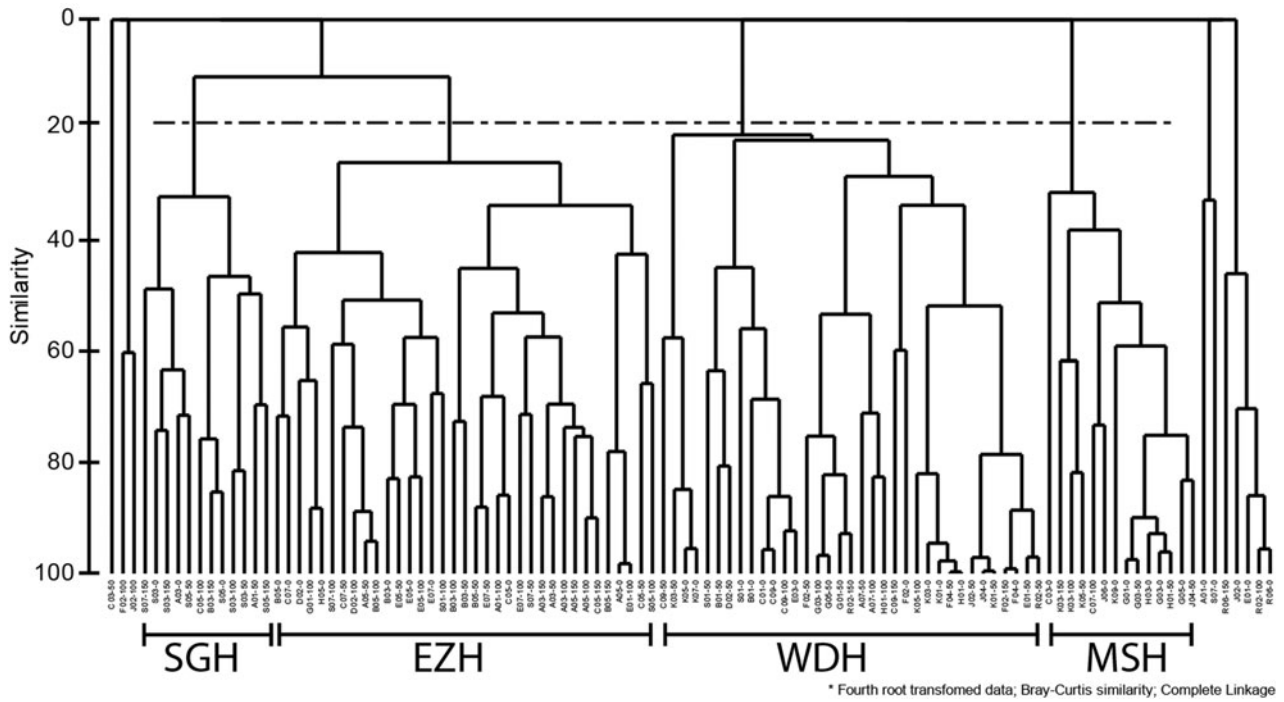


Fig. 6. Dendrogram based on Bray – Curtis similarities (complete linkage, data fourth-root-transformed). The 20% cut line defines four main larval fish habitats: SGH, Southern Gulf Habitat; EZH, Eddy Zone Habitat; WDH, Wide Distribution Habitat; MSH, Mainland Shelf Habitat.

habitat had the lowest mean abundance per sample (220.5 larvae/10 m²), and the second lowest species richness ($d = 0.32$) and diversity ($H' = 0.48$), but dominance ($\lambda = 0.73$) was the second highest of all habitats (Supplementary Material IV).

At the surface (0–50 m), the Mainland Shelf Habitat was located close to the north-east coast over the continental shelf and slope, stretching towards Angel de la Guarda Island with increasing depth (Figure 8). The distribution of the Mainland Shelf Habitat was spatially similar to that of

physical variables (isotherm of 16°C and oxypleth of 4.5 ml/l in the upper strata), and the southern limit was defined by a change of salinity (from 35.3 to 35.2) between the southern tip of Angel de la Guarda Island and the western tip of Tiburon Island (Figure 8E). With our sampling grid it was not possible to identify how far north this habitat extended, but at greater depths the western distribution limit seemed to be the shelf slope. In the upper strata (0–50 m), the 16°C isotherm coincided with the southern distribution limit, as

Table 1. Results of the distance-based linear model between environmental variables and larval fish habitats.

Selection criterion:	R^2	Best Solution:				
Selection procedure:	Step-wise	4 variables	$R^2 = 0.30518$	RSS = 185410		
Total SS(trace):	2.67E + 05					
MARGINAL TESTS						
	SS(trace)	Pseudo-F	P	Prop.		
HMIX	18781	7.8736	0.0003	0.07038		
Temperature	7784.1	3.1248	0.0233	0.02917		
Salinity	35155	15.78	0.0001	0.13174		
Oxygen	29017	12.688	0.0001	0.10874		
SEQUENTIAL TESTS						
	R^2	SS(trace)	Pseudo-F	P	Prop.	Cumul.
Salinity	0.13174	35155	15.78	0.00010	0.13174	0.13174
Temperature	0.23249	26886	13.521	0.00010	0.10075	0.23249
Oxygen	0.29338	16248	8.789	0.00010	0.06089	0.29338
HMIX	0.30518	3148.4	1.715	0.12400	0.01180	0.30518
% OF VARIATION EXPLAINED BY INDIVIDUAL AXES						
Out of fitted model			Out of total variation			
Axis	Individual	Cumulative	Individual	Cumulative		
1	85.25	85.25	26.02	26.02		
2	9.16	94.41	2.8	28.81		
3	5.26	99.67	1.61	30.42		
4	0.33	100	0.1	30.52		

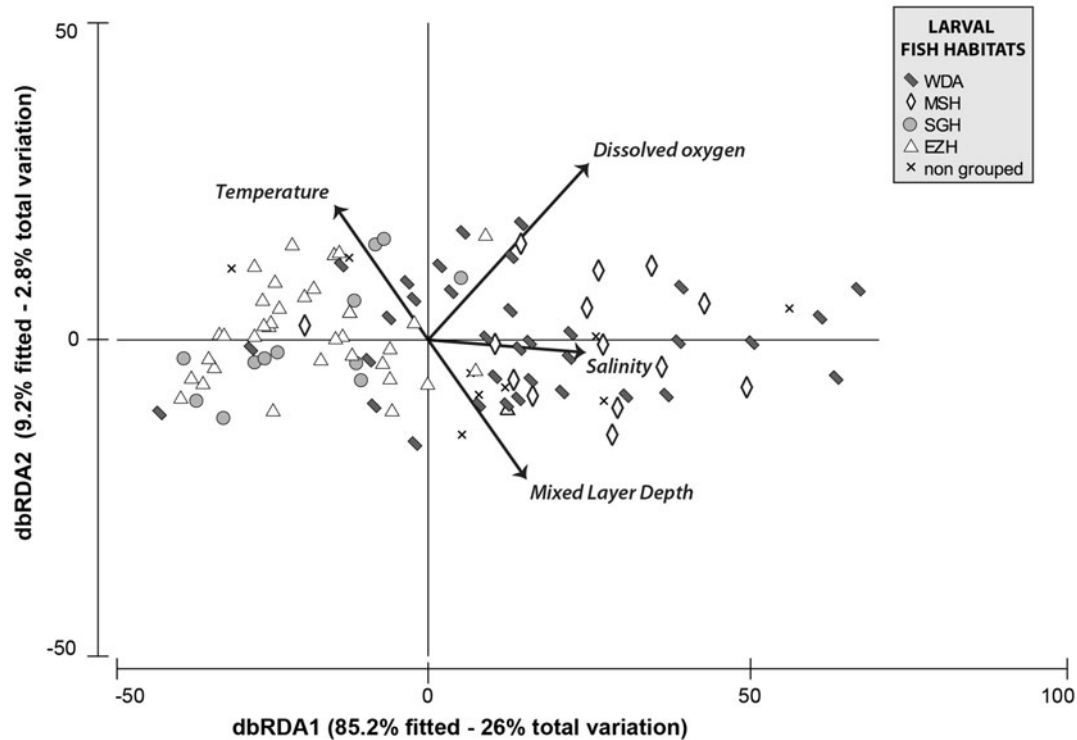


Fig. 7. Plot of the db-RDA showing the relationship between environmental variables and larval fish habitats (LFHs) in the Midriff Archipelago Region of the Gulf of California during winter 2007.

was also the case of the 15°C isotherm in the 50–100 m stratum (Figure 8A, B). The Mainland Shelf Habitat was characterized by and well-oxygenated waters (>5–3.5 ml/l) coming from the north of the GC, and a deep mixed layer (down to 80 m) (Figure 8I–J).

WIDE DISTRIBUTION HABITAT

The second northern LFH, called Wide Distribution Habitat, included 35 samples located from the north to the south limits of the sampled area, from 200 m depth to the surface. It was composed of 13 taxa, with the three main species having pelagic habits (two epipelagic, one mesopelagic). The average similarity among samples within this group was 53.2% (Table 2). The Wide Distribution Habitat was dominated by the widely distributed species *E. mordax* (Supplementary Material II A–D), which had a mean abundance of 491.01 larvae/10 m² and contributed 89.8% to the habitat identity (Table 2). *Leuroglossus stilbius* contributed 4.6% to the group identity, with a mean abundance of 4.47 larvae/10 m² (maximum abundances from 50 to 150 m depth; Supplementary Material III I–L) and a distribution extending to the south. The Wide Distribution Habitat had the highest mean abundance per sample (520.9 larvae/10 m²) and the highest dominance ($\lambda = 0.74$), but the lowest species richness ($d = 0.31$) and diversity ($H' = 0.47$) (Supplementary material IV).

The Wide Distribution Habitat exhibited the widest distribution, both in the north and in the south, and it was the only LFH that crossed the low SST zone (vertical mixing zone), apparently with no limits associated to the physical variables (Figures 7 and 8). In this LFH, the lowest larval abundance was observed in the deeper strata (from 100–200 m) over the vertical mixing zone. Temperatures in the Wide Distribution Habitat ranged from 13.5°C to 17°C, and salinity

from 35.2 to 34.9, including high salinity water from the northern GC, as well as the lowest salinity in the tidal-mixing zone (Figure 8). Dissolved oxygen, ranging from 1.5 ml/l to >5 ml/l, was not a restriction in its distribution either (Figure 8 I–K). The mixed layer reached its maximum depth in this habitat, ranging from 40 m to 110 m (Figure 2D).

EDDY ZONE HABITAT

One of the two southern LFHs, named the Eddy Zone Habitat, was defined in the area influenced by the anticyclonic eddy, from 200 m depth to the surface (Figure 8). The habitat included 35 samples and it was composed of 14 taxa; the principal four species had pelagic habits (three mesopelagic, one epipelagic), and only three had demersal habits. The average similarity among samples was 56.7% (Table 2). *Leuroglossus stilbius* contributed 46.2% to the habitat identity, with a mean abundance of 313.86 larvae/10 m². This species was mainly distributed in the warm side of the south front and in the south zone, with only a few larvae crossing the south front and the sills below 100 m depth (Supplementary Material III I–L). *Diogenichthys laternatus* contributed 37.6% to the group identity, with a mean abundance of 88.80 larvae/10 m², and was exclusively distributed south of the front (Supplementary Material V A–D). The Eddy Zone Habitat exhibited the highest mean species richness ($d = 0.58$) and diversity ($H' = 0.81$), and also a high mean abundance (520.6 larvae/10 m²). It was the habitat with the lowest dominance ($\lambda = 0.57$) (Supplementary Material IVI).

While being spatially coincident with the anticyclonic eddy between 0 and 100 m, this habitat remained through the sampled water column, and its distribution expanded north of the south front at 100–150 m depth, suggesting a northward dispersion at this depth. It also expanded to the south, closely related to the distribution of *D. laternatus* and

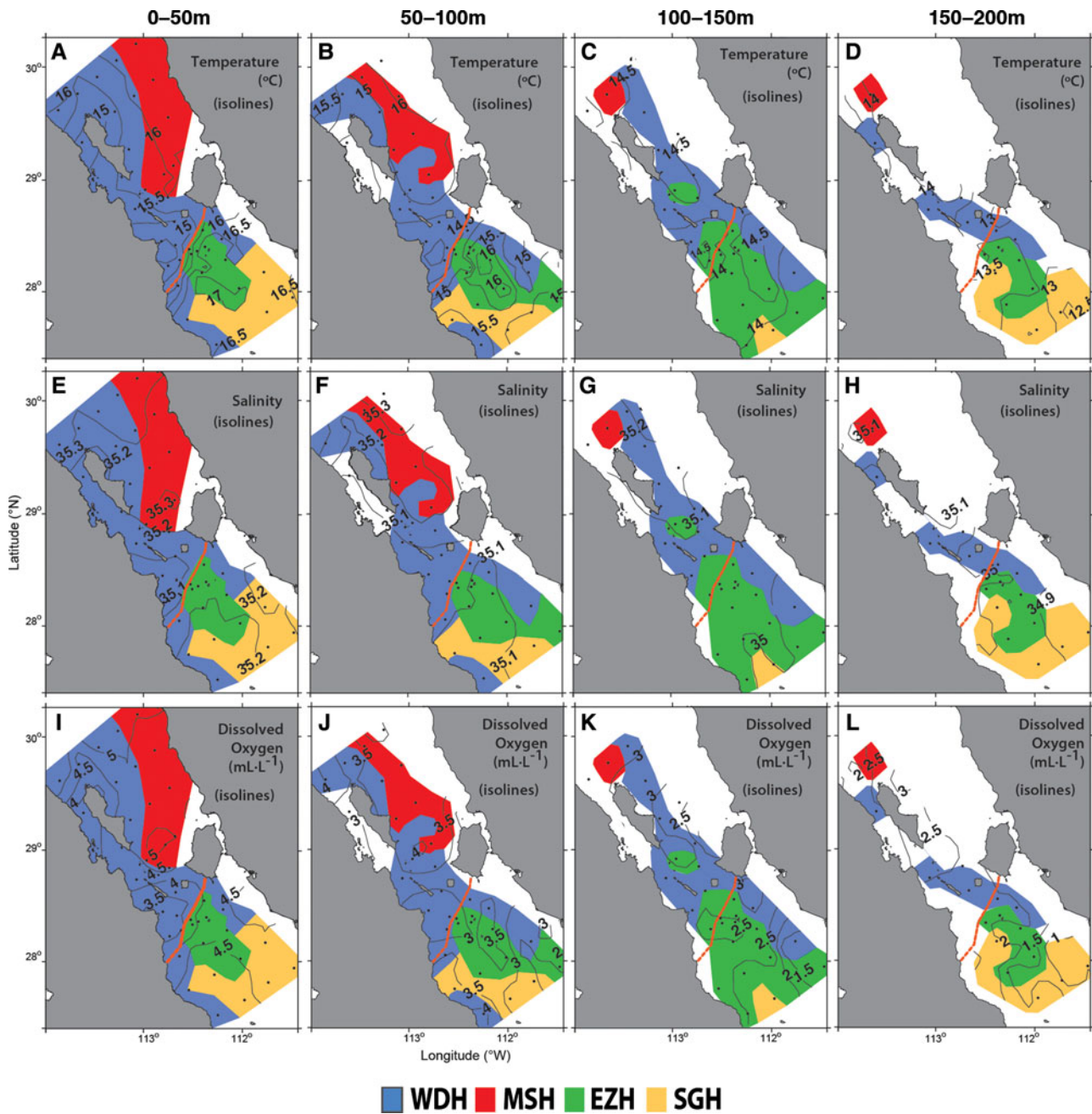


Fig. 8. Larval fish habitats (LFHs, hatch coded) in 50 m depth intervals from 0 to 200 m in relation to hydrographic parameters (isolines): (A–D) mean temperature ($^{\circ}\text{C}$); (E–H) mean salinity; (I–L) mean dissolved oxygen concentration (ml/l). Hatch code for LFHs: small dots, Wide Distribution Habitat; diagonal lines, Mainland Shelf Habitat; shaded horizontal lines, Eddy Zone Habitat; squared, Southern Gulf Habitat. The thick dashed line indicates the position of the south front.

L. stilbius at these depths (Supplementary Material III and VI–L and VI A–D). Temperatures in the Eddy Zone Habitat ranged from $>17^{\circ}\text{C}$ in the surface stratum to 13°C in the deepest stratum (150–200 m) (Figure 8A–D), salinity values ranged from 35.2 to 34.9 (Figure 8E–H) and dissolved oxygen values from 4.5 to >1.5 ml/l (Figure 8I–L).

SOUTHERN GULF HABITAT

The Southern Gulf Habitat contained the lowest number of samples (12), and its distribution was restricted to the south, from 200 m depth to the surface (Figure 8). Samples of the Southern Gulf Habitat had 54.9% of average similarity (Table 2) and were composed of nine different taxa, mainly of

species with pelagic adult habits (epipelagic and mesopelagic). *Leuroglossus stilbius* contributed 72.7% to the group identity with a mean abundance of 236.72 larvae/10 m². *Sardinops sagax* contributed 14.7% (39.71 larvae/10 m²), and *Scomber japonicus* (Houttuyn, 1782) contributed 7.5% (15.67 larvae/10 m²). The distribution of *L. stilbius* and the latter two species are shown in Supplementary Material III (I–L) and Supplementary Material V E–L, respectively. The Southern Gulf Habitat exhibited intermediate species richness ($d = 0.51$), diversity ($H' = 0.69$), and dominance ($\lambda = 0.63$). Mean abundance per sample (297.6 larvae/10 m²) was notably lower than that of its closest habitat (Eddy Zone Habitat; Supplementary Material IV).

Table 2. Contribution of the characteristic fish species to the different larval fish habitats.

	Av. Ab.	Av. Sim	Sim/SD	Contr %	Cum.%
Eddy Zone Habitat					Av. Sim.: 56.7
<i>Leuroglossus stilbius</i>	3.47	26.2	2.51	46.2	46.2
<i>Diogenichthys laternatus</i>	2.64	21.33	4.09	37.61	83.81
<i>Engraulis mordax</i>	1.7	6	0.61	10.58	94.39
<i>Vinciguerria lucetia</i>	0.54	1.05	0.28	1.86	96.25
<i>Sardinops sagax</i>	0.62	0.88	0.25	1.56	97.81
<i>Citharichtys fragilis</i>	0.44	0.66	0.25	1.17	98.98
<i>Scomber japonicus</i>	0.34	0.4	0.18	0.71	99.69
<i>Physiculus rastrelliger</i>	0.16	0.09	0.07	0.15	99.84
<i>Triphoturus mexicanus</i>	0.16	0.05	0.07	0.1	99.94
<i>Entrumeus teres</i>	0.13	0.02	0.04	0.03	99.97
<i>Sebastes</i> sp. 3	0.09	0.02	0.04	0.03	100
Southern Gulf Habitat					Av. Sim.: 54.90
<i>Leuroglossus stilbius</i>	3.4	39.93	2.91	72.72	72.72
<i>Sardinops sagax</i>	1.39	8.06	0.82	14.68	87.4
<i>Scomber japonicus</i>	0.95	4.13	0.52	7.52	94.93
<i>Benthoosema panamense</i>	0.68	2.14	0.31	3.91	98.83
<i>Citharichtys fragilis</i>	0.42	0.64	0.22	1.17	100
Wide Distribution Habitat					Av. Sim.: 53.17
<i>Engraulis mordax</i>	3.45	47.75	2.83	89.79	89.79
<i>Leuroglossus stilbius</i>	0.6	2.46	0.31	4.63	94.42
<i>Sardinops sagax</i>	0.66	1.89	0.28	3.56	97.98
<i>Citharichtys fragilis</i>	0.48	0.85	0.22	1.6	99.58
<i>Sebastes</i> sp. 3	0.18	0.1	0.07	0.19	99.78
<i>Diogenichthys laternatus</i>	0.09	0.03	0.04	0.06	99.84
<i>Hippoglossina stomata</i>	0.09	0.03	0.04	0.06	99.9
<i>Triphoturus mexicanus</i>	0.11	0.03	0.04	0.05	99.95
<i>Trachurus symmetricus</i>	0.13	0.03	0.04	0.05	100
Mainland Shelf Habitat					Av. Sim.: 65.31
<i>Engraulis mordax</i>	3.06	35.61	1.77	54.52	54.52
<i>Citharichtys fragilis</i>	1.78	28.73	4.28	43.99	98.52
<i>Merluccius productus</i>	0.38	0.72	0.18	1.11	99.63
<i>Diogenichthys laternatus</i>	0.24	0.24	0.1	0.37	100

The Southern Gulf Habitat was restricted to the southern zone of the study area, defined by waters of the southern GC (Figure 8). Temperature ranged from 12.5°C to 16.5°C and salinity ranged from 35.2 to 34.9, values typical of the southern Gulf. Dissolved oxygen values ranged from >4.5 ml/l in the upper stratum to >1 ml/l at 150–200 m.

DISCUSSION

The cruise data that support this study represents the hydrography and dynamics of the GC during winter. One of the most important characteristics of the Gulf is its seasonality, both in circulation and hydrography (e.g. Lavín & Marinone, 2003; Palacios-Hernández et al., 2006; Sánchez-Velasco et al., 2009). Although there are very few biological studies, they have revealed that the biological response, indicated by fish larvae, is also seasonal (Moser et al., 1974; Sánchez-Velasco et al., 2009; Peguero-Icaza et al., 2010). The dominant species have a seasonal spawning period, as in the case for the dominant species registered in this study: *Engraulis mordax*, *Citharichtys fragilis*, *Leuroglossus stilbius* and *Sardinops sagax*. These species spawn from the last days of November to the spring months (Green-Ruiz & Hinojosa-Corona, 1997; Hammann et al., 1998; Moser et al., 1974; Aceves et al., 2009; Sánchez-Velasco et al., 2009). Therefore,

this study is representative of winter, and shows relations between the mesoscale hydrographic structures and the fish larval habitats, which were not known.

The physical characteristics of the tidal-mixing frontal zone showed different conditions at each side of the front. South of the front there is a warmer and more stratified water column, in contrast to the colder mixed structure north of the front. These physical contrasts generated the different biological responses: two LFHs were defined in the northern side (Mainland Shelf and Wide Distribution Habitats) and two in the southern side (Southern Gulf and Eddy Zone Habitats) of the front. In each LFH, the dominance and the species contribution were different, which resulted in general patterns of abundance and diversity.

Hydrographic structures, abundance and diversity patterns

The patterns of fish larval abundance and species richness observed in the present study may be indicative of the influence of the mesoscale structures: very high values of both variables occurred inside and on the periphery of the anticyclonic eddy associated with the front from 0 to 100 m depth (Stations A05, B03, B05 and E07), probably due to larval retention by frontal convergence and eddy trapping. This accords with results for the Gaspé Current front in the Mediterranean Sea, where the highest values of zooplankton biomass and fish larval abundance were found in the eddy associated with the front (Fortier et al., 1992), and with more recent studies that have shown that mean larval fish densities were higher in the boundaries of mesoscale anticyclonic features in the Gulf of Mexico (Lindo-Atichati et al., 2012) and in the GC (Contreras-Catala et al., 2012). Although high larval abundance associated with the eddy occurred across all depth strata, specific richness did not, but decreased with depth, where the dissolved oxygen concentrations were also reduced. The larval community below 100 m depth was dominated by *Leuroglossus stilbius* and *Diogenichthys laternatus*, which may be able to resist hypoxic conditions (<1 ml/l). The concentration of 1 ml/l as critical oxygen concentration for zooplankton has also been reported for euphausiid larvae in the tropical–subtropical transitional zone in the southern GC (Tremblay et al., 2010) and for fish larvae of mesopelagic species, such as *Diogenichthys atlanticus* Tåning, 1928 and *Vinciguerria nimbaria* (Jordan & Williams, 1895), off the Angolan coast (John et al., 2001).

The other high larval-abundance spot in the north (30°N 113.5°W) showed a different pattern: high abundance occurred only from 0 to 100 m depth, coinciding with the depth of the mixed layer (80–100 m). Species richness at this site was low, probably as a consequence of unfavourable conditions for the spawning of the fish species that inhabit this area. *Engraulis mordax* was the only frequent species with a wide distribution and no apparent distribution limits; however, its preferred habitat was in the first 100 m of the water column, in accordance with previous studies in the GC (Inda-Díaz et al., 2010) and in other ecosystems (Somarakis & Nikolioudakis, 2010).

Hydrography and larval fish habitats

The Mainland Shelf Habitat, restricted to the mainland continental shelf, east of Angel de la Guarda Island, probably forms

part of the winter southernmost expansion of the summer Shelf Habitat in the upper GC described by Sánchez-Velasco *et al.* (2012). It was composed, among others, of north-exclusive species, such as *Merluccius productus* and *Brosmophycis marginata* (Ayres, 1854), usually found in the north GC (Sánchez-Velasco *et al.*, 2009, 2012). In addition to the high larval abundance of *E. mordax*, the highest abundance of *Citharichthys fragilis* (a pleurinctiform that lives close to the continental shelf) and the presence of *M. productus* contributed to the formation of this habitat. The weak southward current in the north zone of the study area may have retained fish larvae, keeping them away from the turbulent cool mixing zone over the sills; this may result in the formation and maintenance of the Mainland Shelf Habitat. Although the speed of the flow was lower than calculated by numerical models, the southward direction was in accordance with previous studies (Marinone & Lavín, 2003; Peguero-Icaza *et al.*, 2011).

The Wide Distribution Habitat (the other northern habitat) occupied a large area from north-west of the study area to south-east, including the strong mixing zone. This habitat was characterized and dominated by *E. mordax*. This species has been shown to inhabit a wide range of environmental conditions, with a preference for cold waters (Green-Ruiz & Hinojosa-Corona, 1997; Sánchez-Velasco *et al.*, 2000). The wide horizontal distribution in the surface mixed layer has also been observed in other engraulid species, such as *Engraulis ringens* (Jenyns, 1842) in the upwelling system off Chile (Landaeta *et al.*, 2008) and *Engraulis encrasicolus* (Linnaeus, 1758) in the Aegean Sea (Somarakis & Nikolioudakis, 2010), indicating that engraulid species exhibit a high adaptability. Given that *E. mordax* larvae were not limited in their distribution by physical barriers, the area of this habitat was shaped by the larval distribution rather than horizontal or vertical environment gradients.

The Eddy Zone Habitat exhibited the highest larval abundance, richness and diversity, through the sampled 200 m of the water column, although the eddy was only ~100 m deep. The richness of the area influenced by the eddy suggests that the environmental conditions were favourable for the larval development of many different fish species. These conditions could be due to trapping of highly productive water from the frontal zone (resulting in high nutrient concentration) and plankton retention by the eddy (Iles & Sinclair, 1982). Although the eddy had relatively weak fronts, it may still represent a horizontal boundary for the Eddy Zone Habitat, as was demonstrated for other anticyclonic and cyclonic eddies in the southern GC (Contreras-Catala *et al.*, 2012; Sánchez-Velasco *et al.*, 2013). Both studies documented that eddies trapped fish larvae of different adult habits (coastal and oceanic) during their formation, the anticyclonic in the centre and the cyclonic at the edge. A similar process was documented by Kasai *et al.* (2002) using drifters and intensive survey transects in the Kuroshio frontal system, demonstrating the entrainment of coastal water into a frontal eddy and enhanced production inside it. In the same system, Nakata (2000) found a high abundance of coastal-spawned anchovy larvae that possibility were transported to the front and subsequently trapped by an eddy with an elevated productivity in the centre. Muhling *et al.* (2007) sampled contiguous cyclonic and anticyclonic eddies on the Australian coast and found a relation between fish larvae assemblages and eddy structures: higher larval abundance and richness were recorded in the

centre, and different larval fish assemblages in the core and at the periphery of the anticyclonic eddy.

The Southern Gulf Habitat, distributed as far north as the south front, was mainly composed of species with tropical and subtropical affinity, like *Scomber japonicus*, *Sardinops sagax* and *L. stilbius*, a mixture of epipelagic and mesopelagic species. The larvae of this habitat did not cross the front, probably because of the intense vertical mixing and the low food availability on the other side of the front. Some characteristic species of the Southern Gulf Habitat were the same south-distributed fish larvae species recorded in front of Bahía de La Paz (Sánchez-Velasco *et al.*, 2006) and in the oceanic region of the Gulf (Aceves-Medina *et al.*, 2009).

Studies on the effects of frontal systems on fish larval distribution have been carried out mostly during stratification periods (Moser & Smith, 1993; John *et al.*, 2001). Our results indicate that despite the weak stratification and low thermal contrast across the south front compared to summer, it may also function as a three-dimensional boundary between north and south LFHs. This agrees with the findings by Inda-Díaz *et al.* (2010) who documented that *S. sagax* and *E. mordax* responded differentially to the frontal zone in winter. Therefore, we can propose that the front delimits the habitat distribution of the lower trophic levels of the marine food chain both in summer and winter. To understand the importance of the frontal zone for fish larvae distribution, development and subsequent recruitment, more studies are needed to document the seasonal evolution of the south front in the GC on the one hand, and in other frontal systems where similar conditions may occur (e.g. Ensenada front, Angola front).

CONCLUSIONS

We found three-dimensional LFHs whose distribution was shaped by the tidal-mixing front (and associated hydrographic structures) in the MAR in the GC during winter, a period of strong vertical mixing and weak horizontal gradients.

Two northern LFHs were defined: (1) the Mainland Shelf Habitat, located from 0–100 m on the north-east shelf, characterized mainly by the presence of *Citharichthys fragilis*; and (2) the Wide Distribution Habitat, extending from north-west to south across the front, from 0–200 m, dominated by *Engraulis mordax*.

Two southern LFHs were identified south of the front: (3) the Southern Gulf Habitat, occupying the top 200 m in the southern sector of the study area, dominated by *Scomber japonicus* and *Sardinops sagax*; and (4) the Eddy Zone Habitat, associated with the anticyclonic eddy area, exhibiting the highest larval abundance and richness from 0–100 m, dominated by *Leuroglossus stilbius*.

In the present study we demonstrated that even during the winter season hydrographic structures play a key role in the formation of suitable habitats for fish larval development. This suggests that frontal zones, like the one described for the MAR in the GC, are highly important for the creation and maintenance of suitable habitats for fish larvae.

ACKNOWLEDGEMENTS

We would like to thank Alberto Amador, Víctor Godínez, Arturo Ocampo, and Carlos Cabrera (CICESE), and Alma

Rosa Padilla Pilotze (Instituto de Ciencias del Mar y Limonología, Universidad Nacional Autónoma de México) for their support during the sampling and physical data processing. We thank Mayra Pazos and the Drifter Data Assembly Center (GDP/NOAA) for the handling of the drifter data.

FINANCIAL SUPPORT

This work was made possible by the financial support of SEP-CONACyT (contracts SEP-CONACyT 105922 and D41881-F) and CGPI Instituto Politécnico Nacional (project SIP-IPN 1581-20140539). E.A.I.D. thanks CONACyT-México (162568) and Universidad Autónoma de Nayarit (86950) for providing scholarships for doctoral studies.

SUPPLEMENTARY MATERIAL

Supplementary Material I. List of all species recorded during the sampling period in the Midriff Archipelago Region.

Supplementary Material II. Average dissimilarity based on SIMPER analysis between samples of different larval fish habitats. WDH, Wide Distribution Habitat; MSH, Mainland Shelf Habitat; EZH, Eddy Zone Habitat; SGH, Southern Gulf Habitat.

Supplementary Material III. Fish larval abundance in 50 m depth intervals from 0 to 200 m of selected species. A–D, *Engraulis mordax*; E–H, *Cytharichthys fragilis*; I–L, *Leuroglossus stilbius*.

Supplementary Material IV. Characterization of the different larval fish habitats (LFH) by ecological indices.

Supplementary Material V. Fish larval abundance in 50 m depth intervals from 0 to 200 m of selected species. A–D, *Dyogenichthys laternatus*; E–H, *Sardinops sagax*; I–L, *Scomber japonicus*.

The supplementary material referred to in this article can be found online at journals.cambridge.org/mbi.

REFERENCES

- Aceves-Medina G., Jiménez-Rosenberg S.P.A., Hinojosa-Medina A., Funes-Rodríguez R., Saldierna-Martínez R.J. and Smith P.E. (2004) Fish larvae assemblages in the Gulf of California. *Journal of Fish Biology* 65, 832–847.
- Aceves-Medina G., Palomares-García R., Gómez-Gutiérrez J., Robinson C.J. and Saldierna-Martínez R.J. (2009) Multivariate characterization of spawning and larval environments of small pelagic fishes in the Gulf of California. *Journal of Plankton Research* 31, 1283–1297.
- Alvarez-Borrego S. and Lara-Lara J.R. (1991) The physical environment and primary productivity of the Gulf of California. In Simoneit B.R.T. and Drophin J.P. (eds) *The gulf and peninsular province of the Californias. Memoir 47*. Tulsa, OK: American Association of Petroleum Geologists, pp. 555–567.
- Anderson M., Gorley R., Clarke K. (2008) *PERMANOVA for PRIMER: Guide to software and statistical methods*. Plymouth: PRIMER-E Ltd, 214 pp.
- Argote M.L., Amador A., Lavín M.F. and Hunter J.R. (1995) Tidal dissipation and stratification in the Gulf of California. *Journal of Geophysical Research* 100, 16103–16118.
- Bakun A. (1996) *Patterns in the ocean: Ocean processes and marine population dynamics*. La Paz, México: California Sea Grant College System, National Oceanic and Atmospheric Administration in cooperation with Centro de Investigaciones Biológicas del Noroeste.
- Bruce B.D., Evans K., Sutton C.A., Young J.W. and Furlani D.M. (2001) Influence of mesoscale oceanographic processes on larval distribution and stock structure in jackass morwong (*Nemadactylus macropterus*: Cheilodactylidae). *ICES Journal of Marine Science* 58, 1072–1080.
- Clarke K.R. and Ainsworth M. (1993) A method of linking multivariate community structure to environmental variables structure. *Marine Ecology Progress Series* 92, 205–219.
- Clarke K.R. and Warwick R.M. (2001) *Change in marine communities: an approach to statistical analysis and interpretation*. Plymouth: PRIMER-E Ltd.
- Contreras-Catala F., Sánchez-Velasco L., Lavín M.F. and Godínez V.M. (2012) Three-dimensional distribution of larval fish assemblages in an anticyclonic eddy in a semi-enclosed sea (Gulf of California). *Journal of Plankton Research* 34, 548–562.
- Costello M. (2009) Distinguishing marine habitat classification concepts for ecological data management. *Marine Ecology Progress Series* 397, 253–268.
- Danell-Jiménez A., Sánchez-Velasco L., Lavín M.F. and Marinone S.G. (2009) Three-dimensional distribution of larval fish habitats across a surface thermal/chlorophyll front in a semi-enclosed sea. *Estuarine, Coastal and Shelf Science* 85, 487–496.
- Doyle M.J., Morse W.W. and Kendall A.W. (1993) A comparison of larval fish assemblages in the temperate zone of the Northeast Pacific and Northwest Atlantic Oceans. *Bulletin of Marine Science* 53, 588–644.
- Field J.G., Clarke K.R. and Warwick R.M. (1982) A practical strategy for analysing multispecies distribution patterns. *Marine Ecology Progress Series* 8, 37–52.
- Fortier L., Levasseur M., Drolet R. and Theriault J. (1992) Export production and the distribution of fish larvae and their prey in a coastal jet frontal region. *Marine Ecology Progress Series* 85, 203–218.
- García-Córdova J., Peguero-Icaza M., Sánchez-Velasco L., Ocampo-Torres A.I., Amador-Buenrostro A., Cabrera-Ramos C., Godínez-Sandoval V.M., Lavín M.F., Padilla-Pilotze A.R., Rentería-Cano M., Futema-Jiménez S. and Cervantes-Duarte R. (2007) *Datos hidrográficos en el Golfo de California durante febrero de 2007. Campaña GOLCA 0702. B/O Francisco de Ulloa*. Departamento de Oceanografía Física, Centro de Investigación Científica y Educación Superior de Ensenada (63343) 115 pp. Available at: http://oceanografia.cicese.mx/reportes/2007/Garcia_et_al_63343.pdf (accessed 24 February 2014).
- Green-Ruiz Y.A. and Hinojosa-Corona A. (1997) Study of the spawning area of the northern anchovy in the Gulf of California from 1990 to 1994, using satellite images of sea surface temperatures. *Journal of Plankton Research* 19, 957–968.
- Hansen D.V. and Poulain P.M. (1996) Quality control and interpolations of WOCE-TOGA drifter data. *Journal of Atmospheric and Oceanic Technology* 13, 900–909.
- Heagney E., Lynch T., Babcock R., Suthers I. (2007) Pelagic fish assemblages assessed using mid-water baited video: standardising fish counts using bait plume size. *Marine Ecology Progress Series* 350, 255–266.
- Iles T.D. and Sinclair M. (1982) Atlantic herring: stock discreteness and abundance. *Science* 215, 627–633.
- Inda-Díaz E.A., Sánchez-Velasco L. and Lavín M.F. (2010) Three-dimensional distribution of small pelagic fish larvae (*Sardinops sagax* and *Engraulis mordax*) in a tidal-mixing front and surrounding waters (Gulf of California). *Journal of Plankton Research* 32, 1241–1254.

- John H., Mohrholz V. and Lutjeharms J.R.E.** (2001) Cross-front hydrography and fish larval distribution at the Angola–Benguela Frontal Zone. *Journal of Marine Systems* 28, 91–111.
- Kasai A., Kimura S., Nakata H. and Okazaki Y.** (2002) Entrainment of coastal water into a frontal eddy of the Kuroshio and its biological significance. *Journal of Marine Systems* 37, 185–198.
- Landaeta M.F., Veas R., Letelier J. and Castro L.R.** (2008) Larval fish assemblages off central Chile upwelling ecosystem. *Revista de Biología Marina y Oceanografía* 43, 569–584.
- Lavín M.F. and Marinone S.G.** (2003) An overview of the physical oceanography of the Gulf of California. In Velasco-Fuentes O., Sheinbaum J. and Ochoa J. (eds) *Nonlinear processes in geophysical fluid dynamics*. Dordrecht: Kluwer Academic Publishers, pp. 173–204.
- Leduc D., Rowden A., Bowden D., Nodder S., Probert P., Pilditch C., Duineveld G., Witbaard R.** (2012) Nematode beta diversity on the continental slope of New Zealand: spatial patterns and environmental drivers. *Marine Ecology Progress Series* 454, 37–52.
- Lindo-Atichati D., Bringas F., Goni G., Muhling B., Muller-Karger F. and Habtes S.** (2012) Varying mesoscale structures influence larval fish distribution in the northern Gulf of Mexico. *Marine Ecology Progress Series* 463, 245–257.
- López M., Candela J. and Argote M.L.** (2006) Why does the Ballenas Channel have the coldest SST in the Gulf of California? *Geophysical Research Letters* 33, 1–5.
- Marinone S.G.** (2003) A three-dimensional model of the mean and seasonal circulation of the Gulf of California. *Journal of Geophysical Research* 108, 3325.
- Marinone S.G. and Lavín M.F.** (2003) Residual circulation and mixing in the large islands region of the central Gulf of California. In: Velasco-Fuentes O., Sheinbaum J. and Ochoa J. (eds.) *Nonlinear processes in geophysical fluid dynamics*. Dordrecht: Kluwer Academic Publishers, pp. 213–236.
- Martínez Flores G., Nava Sánchez E.H. and Zaitsev O.** (2011) Teledetección de plumas de material suspendido influenciadas por escorrentía en el sur del Golfo de California. *Oceánides* 26, 1–18.
- Martínez Sepúlveda M.** (1994) *Descripción de la capa mezclada superficial del Golfo de California*. Ensenada, Baja California: Universidad Autónoma de Baja California.
- McCune B. and Grace J.B.** (2002) *Analysis of ecological communities*. Glendened Beach, OR: MjM Software Design.
- Mijail A.** (2004) *Biodiversidad: aspectos conceptuales, análisis numérico, monitoreo y publicación de datos sobre biodiversidad*. Managua, Nicaragua: Araucaria XXI.
- Moser H.G.** (1996) *The early stages of fishes in the California Current Region*. CALCOFI Atlas No. 33. Lawrence, KS: Allen Press.
- Moser H.G. and Smith P.E.** (1993) Larval fish assemblages and oceanic boundaries. *Fisheries Science* 53, 283–289.
- Muhling B.A., Beckley L.E. and Olivar M.P.** (2007) Ichthyoplankton assemblage structure in two meso-scale Leeuwin Current eddies, eastern Indian Ocean. *Deep-Sea Research Part II: Topical Studies in Oceanography* 54, 1113–1128.
- Nakata H.** (2000) Implications of meso-scale eddies caused by frontal disturbances of the Kuroshio Current for anchovy recruitment. *ICES Journal of Marine Sciences* 57, 143–152.
- Navarro-Olache L.F., Lavín M.F., Álvarez-Sánchez L.G. and Zirino A.** (2004) Internal structure of SST features in the central Gulf of California. *Deep-Sea Research Part II: Topical Studies in Oceanography* 51, 673–687.
- Paden C.A., Abbott M.R. and Winant C.D.** (1991) Tidal and atmospheric forcing of the upper ocean in the Gulf of California: 1. Sea surface temperature variability. *Journal of Geophysical Research* 96, 18337–18359.
- Peguero-Icaza M., Sánchez-Velasco L., Lavín M.F., Marinone S.G. and Beier E.** (2011) Seasonal changes in connectivity routes among larval fish assemblages in a semi-enclosed sea (Gulf of California). *Journal of Plankton Research* 33, 517–533.
- Sánchez-Velasco L., Shirasago B., Cisneros-Mata M.A. and Avalos-García C.** (2000) Spatial distribution of small pelagic fish larvae in the Gulf of California and its relation to the El Niño 1997–1998. *Journal of Plankton Research* 22, 1611–1618.
- Sánchez-Velasco L., Beier E., Avalos-García C. and Lavín M.F.** (2006) Larval fish assemblages and geostrophic circulation in Bahía de La Paz and the surrounding southwestern region of the Gulf of California. *Journal of Plankton Research* 28, 1–18.
- Sánchez-Velasco L., Jiménez-Rosenberg S.P.A. and Lavín M.F.** (2007) Vertical distribution of fish larvae and its relation to water column structure in the southwestern Gulf of California. *Pacific Science* 61, 533–548.
- Sánchez-Velasco L., Lavín M.F., Peguero-Icaza M., León-Chávez C.A., Contreras-Catala F., Marinone S.G., Gutiérrez-Palacios I.V. and Godínez V.M.** (2009) Seasonal changes in larval fish assemblages in a semi-enclosed sea (Gulf of California). *Continental Shelf Research* 29, 1697–1710.
- Sánchez-Velasco L., Lavín M.F., Jiménez-Rosenberg S.P.A., Montes J.M. and Turk-Boyer P.J.** (2012) Larval fish habitats and hydrography in the Biosphere Reserve of the Upper Gulf of California (June 2008). *Continental Shelf Research* 33, 89–99.
- Sánchez-Velasco L., Lavín M.F., Jiménez-Rosenberg S.P.A., Godínez V.M., Santamaría-del-Angel E. and Hernández-Becerril D.U.** (2013) Three-dimensional distribution of fish larvae in a cyclonic eddy in the Gulf of California during the summer. *Deep-Sea Research Part I: Oceanographic Research Papers* 75, 39–51.
- Smith P.E. and Richardson S.L.** (1977) *Standard techniques for pelagic fish egg and larva surveys*. FAO Fisheries Technical Papers 175. Rome: Food and Agriculture Organization of the United Nations.
- Siver P.A. and Lott A.M.** (2012) Biogeographic patterns in scaled chrysophytes from the east coast of North American. *Freshwater Biology* 57, 451–466.
- Sokal R.R. and Rohlf F.J.** (2012) *Biometry: the principles and practice of statistics in biological research*. 4th edition. New York: W.H. Freeman and Co.
- Somarakis S. and Nikoliodakis N.** (2010) What makes a late anchovy larva? The development of the caudal fin seen as a milestone in fish ontogeny. *Journal of Plankton Research* 32, 317–326.
- Tremblay N., Gómez-Gutiérrez J., Zenteno-Savín T., Robinson C.J. and Sánchez-Velasco L.** (2010) Role of oxidative stress in seasonal and daily vertical migration of three krill species in the Gulf of California. *Limnology and Oceanography* 55, 2570–2584.
- and
- Trumpickas J., Mandrak N.E. and Ricciardi A.** (2011) Nearshore fish assemblages associated with introduced predatory fishes in lakes. *Aquatic Conservation: Marine and Freshwater Ecosystems* 21, 338–347.

Correspondence should be addressed to:

E.A. Inda-Díaz
 Universidad Autónoma de Nayarit, Ciencias Biológicas
 Agropecuarias y Pesqueras
 Km. 9 Carretera Tepic-Compostela, Xalisco, Nayarit, México
 63780
 email: eindad@uan.edu.mx